ASIA-PACIFIC JOURNAL OF MOLECULAR BIOLOGY AND BIOTECHNOLOGY

AsPac J. Mol. Biol. Biotechnol. 2025
ISSN: 0128-7451, eISSN: 2672-7277
Vol. 33 (4): 74-93
https://doi.org/10.35118/apjmbb.2025.033.4.07

RESEARCH ARTICLE

Production of silver nanoparticles using a locally isolated Malaysian bacterial strain: A microbial approach for alternative antimicrobial agents

Farah Najwa Nabila Mohd Hatta[a], Patricia Jayshree Samuel Jacob[b], Rosfarizan Mohamad[c,d], Mas Jaffri Masarudin[a,e*]

[a]Department of Cell and Molecular Biology, Faculty of Biotechnology and Biomolecular Sciences, Universiti Putra Malaysia, 43400, UPM Serdang, Selangor, Malaysia
[b]Department of Biosciences, Nilai University, Persiaran Universiti, Putra Nilai, 71800, Nilai, Negeri Sembilan, Malaysia
[c]Department of Bioprocess Technology, Faculty of Biotechnology and Biomolecular Sciences, Universiti Putra Malaysia, 43400, UPM Serdang, Selangor, Malaysia
[d]Bioprocessing and Biomanufacturing Research Complex, Faculty of Biotechnology and Biomolecular Sciences, Putra Infoport-IOI Resort, Jalan Kajang-Puchong, Universiti Putra Malaysia, 43400 UPM Serdang, Selangor, Malaysia
[e]Nanomaterials Synthesis and Characterisation Laboratory, Institute of Nanoscience and Nanotechnology, Universiti Putra Malaysia, 43400, UPM Serdang, Selangor, Malaysia
*Correspondence email: masjaffri@upm.edu.my

Abstract

The overprescription and misuse of antibiotics contribute to rising bacterial resistance, highlighting the need for new antimicrobial strategies. Silver nanoparticles have emerged as promising agents due to their superior efficiency, attributed to a high surface-to-volume ratio. Non-biological methods for producing silver nanoparticles face significant challenges, including tedious processes, high costs, and harmful by-products post-synthesis. This study investigates the extracellular synthesis of silver nanoparticles using a bacterial strain locally isolated from Selangor, chosen for its cost-effectiveness, rapid reduction properties, and eco-friendly residues. 16S rRNA sequencing was conducted to identify the bacterial phylogeny followed by physicochemical characterisation of the silver nanoparticles. Antimicrobial properties were evaluated using disk diffusion and bacterial growth inhibition assays. 16S rRNA sequencing showed high homology to *Bacillus*. UV-vis spectroscopy revealed the formation of nanoparticles with a peak at 420 nm while dynamic light scattering (DLS) revealed a low polydispersity index (0.20) with 139.73±13.63 nm average particle size. Electron microscopy showed spherical nanoparticles, uniformly distributed with an average diameter of <25 nm, and the presence of a capping agent. Elemental dispersive X-ray (EDX) analysis confirmed 27.41% silver content with minimal residues. Antimicrobial testing against *Escherichia coli* DH5-α demonstrated a 0.87±0.12 cm inhibition zone in the disk diffusion assay, and 10% (v/v) silver nanoparticles inhibited bacterial growth by 50% in the growth inhibition assay. The nanoparticles were found to be 1.5 times more effective than non-nano silver derived from silver nitrate ($AgNO_3$). Thus, these bacterial-synthesised silver nanoparticles show potential as an alternative for antimicrobial agent.

Keywords: antibiotic resistance, antimicrobial efficiency, bacterial–synthesised silver nanoparticles, extracellular synthesis

INTRODUCTION

In the past decade, the post-antibiotic era has been recognised as a global threat, with projections indicating it could result in more deaths than all cancers combined by 2050 (Avershina et al., 2021). This phenomenon has primarily arisen due to the improper use and excessive use of antibiotics (Zhu et al., 2022), rapid dissemination of resistant strains across the globe due to high mobility, and the intrinsic adaptability of microorganisms to evolve naturally (Ramamurthy et al., 2022). Therefore, the escalated

Received: 21 January 2025
Accepted: 9 June 2025
Published: 5 December 2025
Published by: Malaysian Society for Molecular Biology and Biotechnology (MSMBB)

antimicrobial resistance has sparked a growing interest in exploring novel or alternative approaches to address this healthcare crisis which can overcome or complement current antibiotic treatments. There has been a growing interest in nanoparticle-based materials for antimicrobial chemotherapy. Particularly, silver nanoparticles have been proposed as promising nanomaterials for alternative antimicrobial agents (Gherasim et al., 2020). Silver has been used since the 19th century to prevent and treat infectious diseases (Abram & Fromm, 2020) and preservation of food and water (Das et al., 2020). The nanoscale dimension of silver nanoparticles enhances antimicrobial efficiency due to its high surface-to-volume ratio (Patel et al., 2021). Furthermore, numerous studies have demonstrated that silver nanoparticles enhance the antimicrobial efficacy of antibiotics through a synergistic interaction (Rodrigues et al., 2024). As a result, the remarkable properties of silver nanoparticles have been widely utilised in applications such as antimicrobial agents, coatings for biomedical devices, drug delivery systems, and imaging probes (Lee & Jun, 2019). Moreover, silver nanoparticles are now widely used in clinical applications, as they can be incorporated into materials such as wound dressings, implants, and medical devices to prevent bacterial infections (Xin et al., 2022).

Conventional methods of silver nanoparticle production, including physical and chemical syntheses, face significant challenges as these methods involve exhausting processes, less cost-effective, and produce harmful post-synthesis by-products. For instance, physical methods such as ball milling (Selvam et al., 2021), laser ablation (Kalai Priya et al., 2021) and matrix sputtering (Linhares et al., 2020) cause agglomeration of nanoparticles (Xu et al., 2020) and require complex equipment and highly external energy inputs are required to reduce particle size in the process of generating nanoparticles which are not economically friendly for industrial scale production (Endres et al., 2021). Chemical routes cause environmental pollution as they produce hazardous by-products due to excessive use of chemicals like sodium borohydride ($NaBH_4$) and sodium dodecyl sulfate (SDS) as stablisers (Rodriguez-Iruretagoiena et al., 2022) or trisodium citrate and ascorbic acid as surfactants (Barani & Mahltig, 2022) during synthesis (Nguyen et al., 2023). These approaches may limit the nanoparticle potential in medical applications and cause environmental pollution due to their toxicity effects (Xu et al., 2020).

Therefore, green synthesis is suggested to overcome the limitations of non-biological methods. Among green synthesis routes, bacterial-mediated synthesis of silver nanoparticles has gained attention for its sustainability, biocompatibility, cost-effectiveness, non-toxicity, and suitability for mass production, as it involves readily made proteins and enzymes that facilitate the silver metals reduction into silver nanoparticles (Mustapha et al., 2022; Soltys et al., 2021). Particularly, cell-free supernatant from silver nanoparticles-producing bacteria comprises various bioactive compounds, such as proteins and enzymes that can play a crucial role in the process of synthesis of silver nanoparticles as reducing agents (Saeed et al., 2020). The entrapment of silver ions (Ag^+) released from silver occurs through electrostatic interactions between the negatively charged carboxylate ions on the bacterial cell surface and the positively charged Ag^+ (Yu et al., 2020). Once Ag^+ is trapped, nicotinamide adenine dinucleotide (NADH)-dependent reductase from the cell-free supernatant plays a key role in the synthesis of silver nanoparticles. In this process, NADH and a proton in the form of hydrogen (H^+) donate electrons to Ag^+, reducing it to elemental silver (Ag^0), which subsequently accumulates as silver nanoparticles.(Ahmed & Ogulata, 2022). In bacterial-mediated synthesis, extracellular synthesis is favored as intracellular synthesis requires additional steps such as ultrasonication (Pan et al., 2020) and the usage of detergents and salts (Gomes et al., 2020) to recover the accumulated nanoparticles from inside the cells which bring major concern for industrial perspectives (Raju et al., 2015). High-speed centrifugation is only required to recover nanoparticles as the pellets can be redispersed in the desired solvents (Jadoun et al., 2022; Xu et al., 2020).

In Malaysia, the production of silver nanoparticles has been explored using soil bacteria due to the vast aquatic ecosystem (Silva et al., 2020). This includes freshwater ecosystems and marine environments cover approximately 39,000 km^2—accounting for over 10% of the total land area (Prabhakaran et al., 2017). Intensive industrial activities have led to higher concentrations of heavy metals in these ecosystems (Mat Lazim et al., 2023) and therefore led to the emergence of new and varied proteins, metabolites, and polysaccharides (Alotaibi et al., 2021). Exploiting these metabolic pathways could facilitate the discovery of innovative methods for nanoparticle generation by breaking down heavy metal pollutants (Mustapha et al., 2022). This study highlights the extracellular synthesis of silver nanoparticles utilising a locally isolated bacterial strain from Bagan Lalang, Selangor, Malaysia. This locally-isolated bacterium from the Malaysian mangrove ecosystem is expected to produce silver nanoparticles

through extracellular synthesis in aerobic condition and exhibiting antimicrobial properties, making it a suitable candidate for an alternative antimicrobial agent.

MATERIALS AND METHODS

Screening for positive isolate of bacterial-synthesised silver nanoparticles from mangrove soil sediment samples

The bacteria samples were previously sampled (Jacob, 2019) and the positive isolates were screened with modifications (Ghareib et al., 2016) from Bagan Lalang, Selangor, Malaysia at coordinates 5.4333°N and 100.3833°E. Briefly, a single 24 hour-old colony was inoculated from silver nanoparticles-producing bacteria plate originated from the mangrove soil sediment samples. The culture was grown in 100 mL of Luria Bertani (LB) broth (Merck Millipore, USA) in a 250 mL Erlenmeyer flask and then incubated in an orbital shaker set at 150 rpm for 24 hours at room temperature, until the culture became turbid. The culture was subsequently centrifuged at 2600 xg for 30 min at room temperature. Meanwhile, the $AgNO_3$ precursor (Sigma-Aldrich, Germany) with final concentration of 1 M was freshly prepared prior to addition to the cell-free supernatant by adding 0.17 g $AgNO_3$ to 1 mL of sterile deionised water. The 1 mL of 1 M $AgNO_3$ solution was resuspended well and filter-sterilised using 0.45 μm membrane filter. After 30 min of centrifugation, approximately 90 mL of cell-free supernatant was then transferred equally into two sterile 50 mL Falcon tubes. Filter-sterilised 1 M $AgNO_3$ (Sigma-Aldrich, Germany) precursor was added drop by drop to the cell-free supernatant, reaching a final concentration of 10 mM. The $AgNO_3$ solution was also prepared as control. All reaction mixtures were incubated at room temperature for 72 hours with agitation at 150 rpm.

Phylogenetic identification of silver nanoparticles-producing bacteria using 16s rRNA sequencing

The positive strain was further characterised phylogenetically through 16s rRNA sequencing (Mathivanan et al., 2019) with some modifications. The gene of silver nanoparticles-producing bacteria was isolated and amplified using colony PCR with universal bacterial primers synthesised from Integrated DNA Technologies (IDT), Singapore: 27f (5'- AGAGTTTGATCCTGGCTCAG-3') and 1492r (5'-TACGGTTACCTTGTTACGACTT-3') to bind with the conserved regions. The PCR reaction mixture was prepared under cold conditions and included 50 ng of genomic DNA from crude bacterial lysate, 10 pmol each of forward and reverse primers, 400 μM of each deoxynucleotides triphosphates (dNTP) purchased from Geneaid, Taiwan, 0.75 μL of Taq DNA polymerase (Qiagen, Germany), PCR buffer, and 1.5 mM magnesium chloride ($MgCl_2$). The PCR program consisted of an initial denaturation step at 95˚C for 5 minutes (1 cycle), followed by 30 cycles of denaturation at 95˚C for 45 seconds, annealing at 51˚C for 15 seconds, and extension at 72˚C for 2 minutes. A final extension step was performed at 72˚C for 10 minutes (1 cycle). The amplified DNA products were visualised using gel electrophoresis on a 1% (w/v) agarose gel, alongside a GeneDirex 1kb DNA ladder, at 90 V for 30 minutes. The purified PCR products were then sequenced using the forward primer 518F (5'-CCAGCAGCCGCGGTAATACG-3') and reverse primer 800R (5'-TACCAGGGTATC TAATCC-3') primers. The amplified 16s rRNA sequences were compared against the GenBank database in NCBI using standard nucleotide Basic Local Alignment Search Tool (BLAST) program to determine similarity percentage. The phylogenetic relationships were constructed using Molecular Evolutionary Genetics Analysis (MEGA) software using the neighbor-joining method.

Physicochemical characterisation analyses of bacterial-synthesised silver nanoparticles

The generation of bacterial-synthesised silver nanoparticles were then harvested and purified with some modifications (Pourali & Yahyaei, 2016). A 1 mL aliquot of the reaction mixture, containing a cell-free supernatant and $AgNO_3$ precursor solution, was transferred into a microcentrifuge tube and centrifuged at 2,000 xg for 5 minutes. The supernatant was then carefully transferred to a fresh microcentrifuge tube and subjected to a second centrifugation at 14,800 xg for 30 minutes. The resulting pellet was resuspended in 1 mL of sterile deionised water and centrifuged again at 14,800 xg for 30 minutes to complete the purification process. The final pellet obtained was then air dried for 48 hours and resuspended in 1 mL sterile deionised water prior to subsequent analyses.

(i) Preliminary screening of bacterial-synthesised silver nanoparticles formation via UV-vis spectrophotometry

An aliquot of 1 mL of cell-free supernatant containing bacterial-synthesised silver nanoparticles until 72-hour incubation into quartz cuvette against LB broth as blank. The OD reading was taken from the range of 250 nm until 600 nm and the graph was plotted to identify the absorbance peak of bacterial-synthesised silver nanoparticles formation with three biological replicates. The statistical significance of absorbance at

the 420 nm wavelength across different time points was evaluated using Two-way Analysis of Variance (ANOVA). A Tukey's Honestly Significant Difference (HSD) post-hoc test was then performed to determine significant pairwise differences in nanoparticle formation at various incubation times. All statistical analyses were conducted using GraphPad Prism 9.5.1 (GraphPad Software, U.S.A.).

(ii) Dynamic Light Scattering (DLS) for the size and monodispersity analysis of bacterial-synthesised silver nanoparticles

The dried pellets of silver nanoparticles were dispersed in 1.5 mL sterile deionised water and sonicated at 30 V for 30 minutes to obtain a homogenous sample followed by filter-sterilised with a Millipore (Merck, Germany) syringe filter with a pore size of 0.22 μm. The solution was aliquoted into 1 mL portions and transferred into a cuvette for analysis, which included determining the nanoparticles' diameter and polydispersity index (PDI) using a Malvern Zetasizer NanoZS instrument (Malvern Instrument, UK). The samples were analysed triplicates and average hydrodynamic diameter together with PDI were determined.

(iii) Particle morphological analysis of bacterial-synthesised silver nanoparticles formation using Field Emission Scanning Electron Microscopy (FESEM)

The size, morphology, and elemental composition of bacterial-mediated silver nanoparticles were analysed using FESEM (FEI Model: NOVA NANOSEM 230, USA) using the method demonstrated by (Chandrakanth et al., 2014) with some modifications. Bacterial-synthesised silver nanoparticles in dried pellet form dispersed in 1 mL of sterilised deionised water, sonicated at 30 V for 30 minutes, and filter-sterilised with a syringe filter with a pore size of 0.1 μm. The solution was then diluted at a 1:50 ratio with deionised water, resulting in a final volume of 1 mL. Then, 10 μL of the diluted nanoparticle solution was dropped onto clean aluminum stubs and dried at 55˚C for 72 hours. Following the drying process, the sample surface was coated with a thin layer of gold using ion beam sputtering. The sample was then mounted on a stage and placed in a high vacuum chamber. Ultra-high magnification, up to 500,000x, with a resolution of 1 nm at 15 kV, was employed to examine the topological features of the bacterial-synthesised silver nanoparticle structure.

(iv) Size, morphological, and elemental composition analysis of bacterial-synthesised silver nanoparticles using Transmission Electron Microscopy–Energy Dispersive X-ray (TEM-EDX) Spectroscopy

The size, morphology, and elemental composition were further analysed using TEM with some modifications (Rauwel et al., 2015). The silver nanoparticle suspension was first filtered using a 0.1 μm filter and then sonicated for 15 minutes in an ultrasonic bath to disperse the nanoparticles. The suspension was then applied dropwise onto a 300 mesh, 3 cm carbon-coated copper grid and left to air-dry for 16 hours. Prepared nanoparticles samples were then viewed and the elemental composition was analysed using a TEM-EDX Model JEM-2100F (JEOL, Munich, Germany) operating at 200 kV at 500 000x magnification. The degree of conversion of silver formula was calculated with modification as the difference between initial concentration and the final concentration of silver (Długosz & Banach, 2019).

$$\frac{Ci\ Ag - Cf\ Ag}{Ci\ Ag}\ x\ 100\%$$

C_i Ag = Atomic weight percentage of Ag in $AgNO_3$ precursor

C_f Ag = Atomic weight percentage of Ag in silver nanoparticles

Evaluating the antimicrobial potential of bacterial-synthesised silver nanoparticles against gram-negative E. coli bacteria

(i) Growth inhibition zones evaluation

The antimicrobial activity of of bacterial-synthesised silver nanoparticles against gram-negative *E. coli* DH5-α bacteria strain was assessed using the Kirby-Bauer disk diffusion method (Bauer et al., 1966), with modifications. A 24-hour-old colony of *E. coli* DH5-α bacteria was grown in LB broth at 37˚C for 24 hours with shaking at 150 rpm. *E. coli* DH5-α cultures with approximately 300 μL were spread on sterile LB agar plates and 5 mm of cellulose disks saturated with sonicated bacterial-synthesised silver nanoparticles suspension was placed on the spread microbial culture. The saturation of 5 mm of cellulose disks with bacterial-synthesised silver nanoparticles suspension was done by immersing 500 μL of sonicated bacterial-synthesised silver nanoparticles suspension for 10 minutes before placed in the centre of the LB agar plate containing *E. coli* DH5-α cultures.

Disks saturated with ampicillin and kanamycin at 2 and 30 μg/mL concentrations respectively were tested as positive controls while blank and distilled water saturated disks were used as the negative controls (Oxoid, USA). Disk immersed with $AgNO_3$ precursor solution with final concentration of 10 mM was also included in the assay. The assay plates were incubated at 37°C for 24 hours. After incubation, the diameter of the inhibition zones was measured and recorded. The experiment was conducted with three biological replicates. A Two-way ANOVA was used to evaluate the statistical significance of the inhibition zones for antimicrobial agents, comparing them to distilled water as a negative control. All analyses were performed using GraphPad Prism 9.5.1 (GraphPad Software, USA). From this data, the rate of efficiency of bacterial-synthesised silver nanoparticles comparing to $AgNO_3$ precursor in normalised concentration was calculated as below:

$$\frac{Zone\ of inhibition\ of\ AgNPs\ (Final) - Zone\ of\ inhibition\ of\ AgNO_3 (Initial)}{Zone\ of\ inhibition\ of\ AgNO_3\ (Initial)}\ x\ 100\%$$

(ii) Bacterial growth inhibition assay

The antimicrobial effect of bacterial-synthesised silver nanoparticles on the growth rate of *E. coli* DH5-α in suspension culture was assessed with three biological replicates using a bacterial growth inhibition assay. A single 24-hour-old colony of *E. coli* DH5-α was inoculated into 100 mL of LB broth in a 250 mL Erlenmeyer flask. Then, 10 mL of the previously grown *E. coli* DH5- α culture was added to 90 mL of fresh LB broth and incubated at 37°C with continuous shaking at 200 rpm. Absorbance at 600 nm was measured every 30 minutes to track the culture's growth and construct the growth curve for *E. coli* DH5-α. The same procedure was repeated with the addition of 1% (v/v) and 10% (v/v) sonicated bacterial-synthesised silver nanoparticles at the bacterial lag and log phases, respectively. A Two-way ANOVA was used to assess the statistical significance of the increase in OD within 300 minutes post-treatment. Subsequently, a Tukey's HSD post-hoc test was performed to identify significant pairwise differences in growth inhibition activity between treated and untreated bacterial cultures. All statistical analyses were conducted using GraphPad Prism 9.5.1 (GraphPad Software, U.S.A.).

RESULTS AND DISCUSSION

Screening and phylogenetic identification of local bacteria capable of silver nanoparticles production

The local bacteria that capable of producing silver nanoparticles have been isolated and further understanding is needed to identify the phylogeny of silver nanoparticles-producing bacteria. Figure 1 shows the colony morphology of silver nanoparticle-producing bacteria grown on Figure 1 (A) LB agar after 18 hours of incubation at room temperature, appearing as milky-white, irregularly shaped colonies with a waxy exterior. Figure 1 (B) demonstrates the extracellular aerobic generation of silver nanoparticles from cell-free supernatant as the reaction mixture color was changed from yellow to dark brown after incubation with 10 mM $AgNO_3$ precursor for 72 hours at room temperature and there were no changes in color for cell-free supernatant without $AgNO_3$ precursor. The color change from yellow to brown is a direct result of the size-dependent optical properties of silver nanoparticles (Link & El-Sayed, 2003). This change serves as an early indication that bacterial-synthesised silver nanoparticles have formed, resulting from the surface plasmon resonance (SPR) phenomenon. In this process, conduction electrons on the nanoparticle surface oscillate collectively in response to incident light, absorbing and scattering specific wavelengths, which causes the color to shift from yellow to brown (Kannan et al., 2010). Furthermore, this process is also involving intensity concentration dependent as the intensity of the brown color of reaction mixture increases over time given a fixed concentration of $AgNO_3$ precursor. The silver reduction process requires a certain length of time for the nucleation process to occur, and for the nanoparticles to grow to the desired size as the time taken for the optimal synthesis of silver nanoparticles from Bacillus cereus isolated from contaminated soil was at 69 hours (Ibrahim et al., 2021). Therefore, the change of color from yellow to darker shade in bacterial nanoparticle synthesis is due to the growth and aggregation of nanoparticles, driven by the reduction of precursor materials by bioactive compounds produced by bacteria.

The 16s rRNA gene of the silver nanoparticle-producing bacterium was amplified, yielding a ~1.5 kb fragment. The fragment was then purified and sequenced to determine the full-length 16s rRNA nucleotide sequence as shown in Figure 1 (C).

Subsequent BLAST analysis against the NCBI 16S rRNA database revealed high similarity to Bacillus species, as supported by the phylogenetic analysis in Figure 1(D), which confirmed that the isolate is closely related to Bacillus spp., particularly B. cereus strain KTSMBNL, B. thuringiensis strain BTJ-S-1, B. cereus strain UITSAI, and B. subtilis strain Mans5. Moreover, silver nanoparticles-producing bacteria are also associated with different genera, such as Enterococcus faecium strains K, IMAU 10052, and PL11; Lactobacillus delbrueckii strain GERU3; and Neobacillus novalis strain HBG31. Studies have shown that several bacterial strains from Bacillus spp. are capable of producing silver nanoparticles, as demonstrated by the use of two mesophilic bacteria, B. indicus and B. cecembensis, (Shivaji et al., 2011). Interestingly, different bacterial strains that have the ability to synthesise silver nanoparticles naturally are isolated from different habitats rather than mangrove environment. For instance, metal resistant B. cereus isolate from electroplating industries in India demonstrating a potential generation of silver nanoparticles (Babu & Gunasekaran, 2009). From this observation, it is concluded the bacteria has been evolved with resistance to heavy metal ions or specifically growing in metal ion rich niche can be used for the purpose of factory for nanoparticles production. Based on the results, the 16S rRNA sequencing successfully narrowed down the identity of the unknown bacterium to the genus level. However, to achieve more precise species-level identification, further studies, such as whole-genome sequencing, could be undertaken for a comprehensive analysis of the organism's entire genetic material, facilitating taxonomic classification by comparing the complete genome to existing databases or reference genomes (Kweon et al., 2020).

Physicochemical characterisation of bacterial-synthesised silver nanoparticles

The color of reaction mixture changed when the cell-free supernatant was incubated with $AgNO_3$ precursor from yellow to dark brown indicated the nanoparticles have been formed by the reduction of NO^- to NO^{2-} and transferring the electron to Ag^+, leading to conversion of Ag^+ to silver nanoparticles (Kalimuthu et al., 2008). However, deeper understanding of color changes in reaction mixture needs to be carried out to characterise the nanoparticles mediated by silver nanoparticles-producing bacteria.

(i) Preliminary assessment of bacterial-synthesised silver nanoparticles using UV-vis spectroscopy

UV–vis absorption spectroscopy is a widely used technique for the initial characterisation of nanoparticle structures, as the absorption bands correlate with the size and aspect ratio of metal nanoparticles. (Smitha et al., 2008). Figure 2 (A) shows the UV-vis absorption peak of bacterial-synthesised silver nanoparticles and Figure 2 (B) the time point absorbance peak at the wavelength of 420 nm. Preliminary determination of bacterial-synthesised silver nanoparticles formation from OD trendline in Figure 2(A) as the cell-free supernatant was incubated with 10 mM $AgNO_3$ precursor and the distinct peak was observed at 420 nm wavelength meanwhile positive control of $AgNO_3$ showed strong peak at the wavelength of 310 nm with lower absorbance value. The increased absorbance seen in bacterial-synthesised silver nanoparticles, compared to the control, is mainly attributed to the formation, growth, and possible aggregation of silver nanoparticles during the synthesis process.The nanoparticle synthesis process by the silver nanoparticles-producing bacteria may result in a higher concentration of nanoparticles in the solution compared to the control, where only $AgNO_3$ is present which therefore contribute to higher absorbance values in the UV-vis spectrum. The absorbance reading shifting from positive control to sample indicates the bacterial-synthesised silver nanoparticles have been formed. The absorption peak of this bacterial-synthesised silver nanoparticles at 420 nm is consistent with previous studies confirming successful production of silver nanoparticles from Streptococcus hygroscopicus showed a prominent and broad peak between 420 nm and 425 nm, which indicates the presence of silver nanoparticles attributed to the reduction of metal ions by secondary metabolites in the cells (Sadhasivam et al., 2010). Similarly, exploitation of Aspergillus niger isolated from the soil (Gade et al., 2008) and Pseudomonas aeruginosa (JQ989348) for silver nanoparticles synthesis showed 420 nm peak respectively (Ramalingam et al., 2014). The raw data of this assay is in Supplementary 1.

A

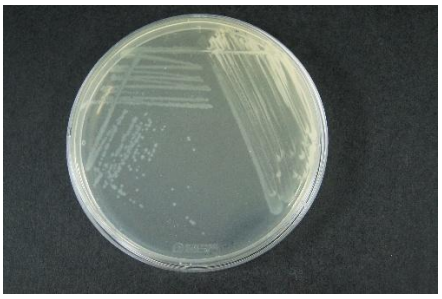

B

Control **72 hours**

C

>Bacterial-synthesised silver nanoparticles
CGGACTTGCAGCGTAATATACATGCAGTCGAGCGAATGGATTAAGAGTTCTC
TTATGAAGTTAGCGGCGGACGGGTGAGTAACACGTGGGTAACCTGCCCATA
AGACTGGGATAACTCGGGAAACCGGGGCTAATACCGGATAACATTTTGAAC
CGCATGGTTCGAAATTGAAAGGCGGCTTCGGCTGTCACTTATGGATGGACC
CGCGTCGCATTAGTCTAGTTGGTGCAGCTAACGGCTCACCAAGGCAACCAT
GCGTAGCCGACCTGAGAGGGTGATCGGCCACACTGGGACTGAGACACGG
CCCAGACTCCTACGGGAGGCAGCAGTACGGAATCTACCGCAATGGACGAA
AGTCTGACGGAGCAACGCCGCGTGAGTGATGAAGGCTATCGGGTCGTAAA
ACTCTGTTGTTAGGGAAGAACAAGTGCTAGTTGAATAAGCTGGCACCTTGA
CGGTACCTAACCAGAAAGCCACGGCTAACTACGTGCCAGCAGCCGCAGTA
ATACGTAGGTGGCAAGCGTTATCCGGAATTACTGGGCGTAAAGCGCCGCGC
AGCTGGTCTTCTCAAGTCTGATTGTGAACAGCCCACGGCTCAACCGCTGGA
GGGTCATTTGAAACTGGGAGACTTGAATGGCAGAAGGAGGAAAGTGGAATT
ACATGTGTACCGGTGAAATGCCGAAAAGATATGGAGGAACCACCAGTAGCG
AAGGCGACTTTTCTGGTCTGTAACCGACACTGAGGCGGCGAAAGCCTGGG
GAGCAAACCAGGATTAGGATACCCTGGTACGTCCACGCCGGAAACGAAGA
AGTGCTTAAGTGTAAGAGGGTTTCCGCCCTTTAGTTGCTGAAGGTTAACCC
ATTAAGCAATTCCCCCTGGGGAGTACCGCCGGCAAGGCTGAAAATCCAAAG
GAAATAGACCGGGGGCCCGCACAGCCGTGGAACCATGTGGTTAAATTCGG
AAGCAACGCGAAGGAACCTTACCAGGTCTGACATCCTCTGGACACCCCAAA
AAATAGGCTTCTCCCTCAGGGAGCAGAATGACCAGTGGTGCCATGGTTGTC
GTTCAGCTCGGGTTCAGTGAGAAGTATGCGTTAAAGTCCTGCCACGAAGCG
CCACCCCTGGATCTTTAGTGACATCATCTAATTGGGCACATCTTAAGGGGAC
TCCCGGGACCAACCGGGAGGAAGCGTGGAGAGGACCTCAAATCATCCATC
ACCCCTTATGACCTTGGCTTCACCACCTTGCTCCAAGGACCGGTCCAAAGA
GCTGCACAGAACCCCCAAGTGGGAAGTTATTTTCAAAAACCCTTTTCCATTT
GGGATGGTAGGTGCCAATTGCCCACCAGGAGGCGGAATTCGTTGGTATTCG
GGATTCACCAGCCCCCGGTAAAAAGTTTCCCGGCCCTGGACACCCCCCCC
CTTCCCACCCCGGAATTTGTAACCCCCGGAGTTGGTTGGGGAACCCTTTG
GAGCCAGCCGCCTAATATAATCAGAGGTTCG

D

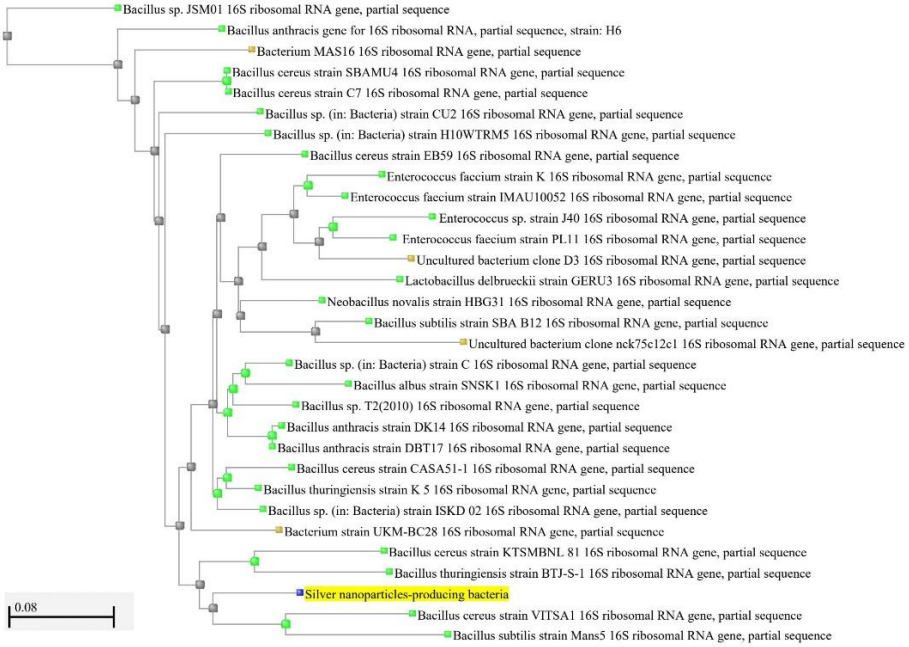

Figure 1. Phylogenetic identification of silver nanoparticles-producing bacteria. (A) Colony of silver nanoparticles-producing produced irregular, milky-white colonies with waxy exterior morphology. (B) Comparison of bacterial-synthesised silver nanoparticles in reaction mixture incubating with 10 mM final concentration of $AgNO_3$ precursor at 72 hours post incubation and cell-free supernatant without precursor as a control. The reaction mixture depicted a change in media color from yellow to dark brown, indicating formation of the nanoparticles. (C) Sequencing result of purified 16s DNA sequence from isolated bacteria. (D) Phylogenetic tree construction of silver nanoparticles-producing bacteria. The isolated bacteria are closely-related to the *Bacillus* spp., as it falls in to *Bacillus* clade.

The incubation time for silver ions from $AgNO_3$ precursor to be converted into silver nanoparticles was depicted in Figure 2 (B). The time point absorbance at the wavelength of 420 nm starting from zero hour to 72 hours as the value trend declines across incubation time. A prolonged incubation time induces nanoparticle aggregation. This phenomenon causes size increment and alters the scattering properties of the nanoparticles, leading to a decrease in the OD reading (Bu & Lee, 2012). In addition, the reaction kinetics may almost reach a saturation point or equilibrium, causing the rate of silver nanoparticles formation to slow down. This could be reflected in a reduction of OD reading as the reaction progresses. This rate of reduction of Ag^+ ions, when limited, directly impacts the OD during the reaction process (Tatarchuk et al., 2013). Extending the incubation time silver nanoparticles formation may cause completion of the reduction reaction, reaching a point of equilibrium where the concentration of reactants and products remains relatively constant. This could result in a plateau OD reading in the graph (Kamala Nalini & Vijayaraghavan, 2020). Other than that, prolonged time of the reaction mixture may not significantly contribute to the formation of silver nanoparticles or improve desired properties in terms of nanoparticle yield or quality. This was supported by a study on silver nanoparticle synthesis using Musa balbisiana leaf extract. The reaction mixture was incubated for a range of zero to 120 hours, revealing that an incubation time of 72 hours is optimal for both the synthesis and stability of the silver nanoparticles. Over time, the color intensity and absorbance at 420 nm gradually increased until the 72-hour timepoint, after which both parameters remained nearly constant (Dave et al., 2022). The raw data of this assay is in Supplementary 2.

(ii) Particle size distribution and polydispersity analysis of bacterial-synthesised silver nanoparticles using DLS

The DLS curve showing silver nanoparticles have been produced as a single and narrow pattern of bell-shaped curve of bacterial-synthesised silver nanoparticles sample indicated a well-defined with less polydisperse nanoparticles as shown in Figure 3 (A). Multiple replicates were performed to ensure reproducibility, as shown in Figure 3(B). DLS measurements gave the value of the PDI and hydrodynamic diameter in z-average (nm) value together with standard deviation (SD) for respective data of the bacterial-synthesised silver nanoparticles. The data was obtained from six biological replicates with three technical replicates each. The raw data is in the Supplementary 3.

Based on Figure 3 (B), the average hydrodynamic diameter was 139.73±13.63 nm, representing the diameter of the nanoparticles that were most abundant in the colloidal solution. The low PDI value of 0.2±0.05 indicates a uniform particle size distribution, reflecting the homogeneity of the nanoparticle sizes. Both results support that the DLS measurements of the bacterial-synthesised silver nanoparticles demonstrate uniform particle size and distribution in the colloidal solution.These findings are comparable to extracellular synthesis of silver nanoparticles by bacteria such as Pseudomonas stutzeri as the silver nanoparticles were built up just about 200 nm in diameter and of a definite composition and shape (Beyene et al., 2017). Salmonella thypirium was proven to biosynthesis of silver nanoparticles as the DLS result showed 129.30 nm size with PDI 0.13 value, indicating monodispersed silver nanoparticles have been formed (Ghorbani, 2013). Other than that, some studies showed lower values with less than 100 nm diameter of silver nanoparticles with less than 0.50 PDI values (Modi et al., 2015).

(iii) Morphological and particle characterisation of bacterial-synthesised silver nanoparticles using FESEM and TEM

Nanoparticle characterisation using FESEM and TEM are the common methods for analysis of surface morphology of nanoparticles. Figure 4 depicts FESEM images of the surface morphology of Figure 4(A) cell-free supernatant of silver nanoparticles-producing bacteria while Figure 4(B) is the $AgNO_3$ precursor diluted with sterile distilled water at 10 mM concentration. The successful formation of bacterial-synthesised silver nanoparticles has shown in Figure 4(C) and Figure 4(D) at two different magnifications. TEM micrographs of bacterial-synthesised silver nanoparticles were shown in Figure 4 (E) and (F) at magnifications of 50 000x and 100 000x respectively using an electron beam accelerating at 100 keV.

A

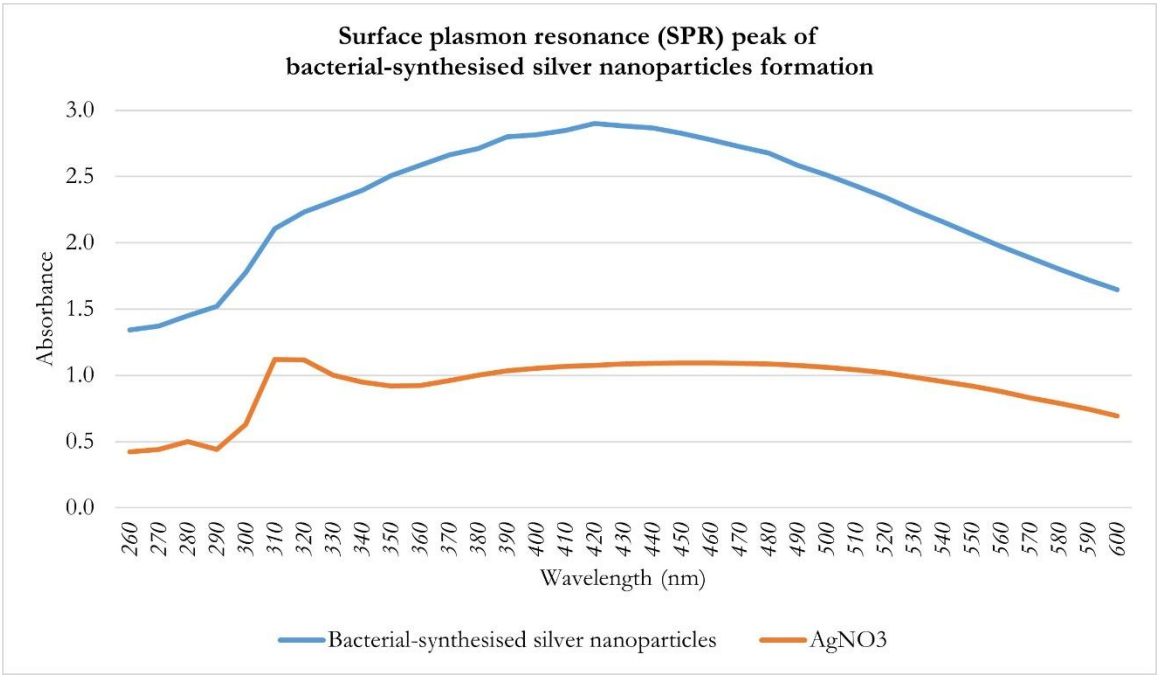

B

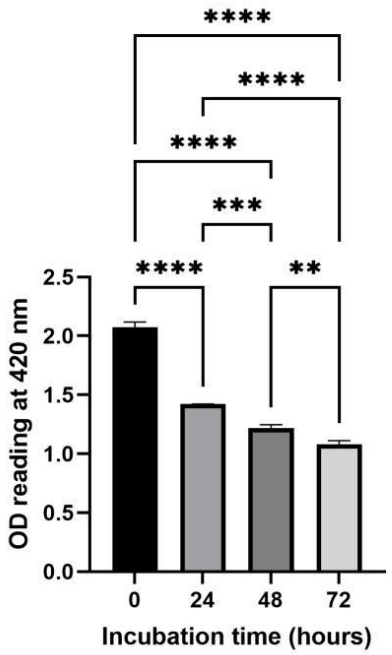

Figure 2. Preliminary assessment of bacterial-synthesised silver nanoparticles formation. The line graph shown in (A) from UV-vis spectroscopy after the cell-free supernatant of bacterial producing silver nanoparticles incubating with 10 mM $AgNO_3$ precursor after 72 hours in a wavelength range of 300 to 600 nm. The distinguishable absorbance peak was observed at around 420 nm for bacterial-synthesised silver nanoparticles meanwhile positive control comprising LB media incubated with 10 mM $AgNO_3$ precursor showed absorbance peak at 310 nm with lower absorbance reading. (B) is the time point absorbance at the wavelength of 420 nm starting from zero hour to 72 hours as the trend declines across incubation time. The symbol of "*" indicates significance with $p < 0.05$; "**": $p < 0.01$; "***": $p < 0.001$; $p < 0.0001$ and ns: not significant.

A

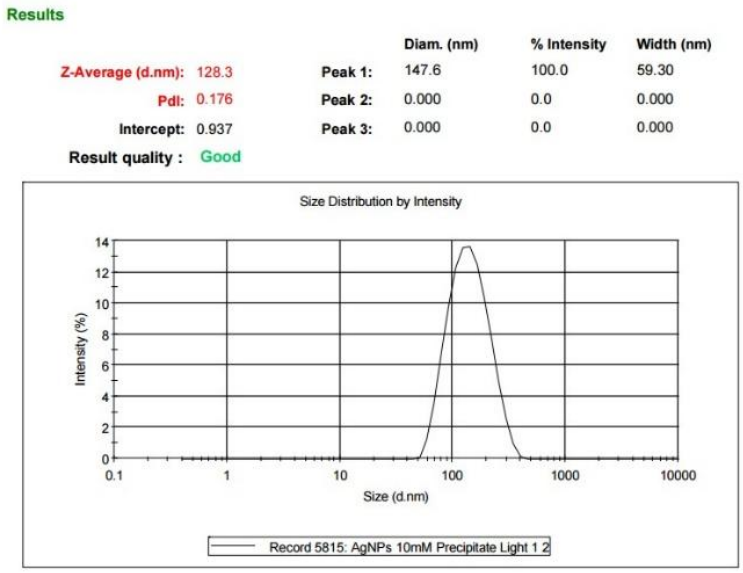

B

AgNPs	z-average (nm)	PDI
B1	146.03	0.21
B2	147.53	0.21
B3	149.50	0.21
B4	127.30	0.18
B5	118.00	0.15
B6	150.03	0.28
Mean	**139.73**	**0.20**
SD	**13.63**	**0.05**

Figure 3. Size and polydispersity of bacterial–synthesised silver nanoparticles analysis in solution via DLS. (A) is the successful formation curve of bacterial-synthesised silver nanoparticles showing size distribution and PDI value and (B) depicted the average of hydrodynamic diameter (nm) and PDI value of bacterial-synthesised silver nanoparticles replicates.

Interpreting from the Figure 4, there are significant morphological trends among all samples. Figure 4 (A) shows a big clump of irregular shape from a cell-free supernatant of silver nanoparticles-producing bacteria meanwhile Figure 4 (B) is the photograph of $AgNO_3$ precursor at 10 mM concentration showing rectangular lattice shape with the size about 1 μm. Figure 4 (C) is the final form of bacterial-synthesised silver nanoparticles with uniform spherical shapes with minor aggregation after incubating the cell-free supernatant with $AgNO_3$ precursor at 10 mM after 72 hours and Figure 4 (D) is the image of bacterial-synthesised silver nanoparticles with higher magnification as we can conclude the size of bacterial-synthesised silver nanoparticles is less than 25 nm with slight differences in range. Ideally, the size of nanoparticles in FESEM should be equivalent with the result of z-average in DLS measurement. However, the FESEM result showed otherwise as the diameter size of bacterial-synthesised silver nanoparticles are smaller than the size depicted in the DLS result. This is due to the aggregation of silver nanoparticles that has occurred in colloidal solution prior to DLS analysis. A closer look at this sample Figure 4 (D) at high magnifications of 200 000x postulates smaller, sphere shaped of bacterial-synthesised silver nanoparticles were observed. These findings are similar to where the hydrodynamic diameter of silver nanoparticles synthesised by B. thuringiensis, E. coli, Staphylococcus aureus, and Salmonella typhimurium from DLS analysis were larger than FESEM results respectively (Verma et al., 2018).

While FESEM offers essential details on nanoparticle shape and surface topology, TEM allows for the visualisation of the cross section of a thin sample using phase contrast imaging (Egerton, 2011). The TEM micrograph of bacterial-synthesised silver

nanoparticles in Figure 4 (E) resembled uniform and monodisperse spherical shape bacterial-synthesised silver nanoparticles surrounded by membrane-like structure produced by silver nanoparticles producing bacteria and (F) depicting the size of bacterial-synthesised silver nanoparticles with less than 20 nm, slightly smaller than FESEM images in Figure 4 (D). Ideally, the size of nanoparticles shown in FESEM should be similar with observations from TEM images. However, the average particle size of bacterial-synthesised silver nanoparticles depicted in FESEM images were slightly greater than the sizes measured in TEM images. This was due to the signals in TEM used for particle size measurement come from the core of the metallic nanoparticles and pass through the surface organic layer. In contrast, FESEM takes into account the organic residues on the nanoparticle surface, which must be considered when measuring the particle size at the surface (Eaton et al., 2017). Another interesting observation in TEM micrographs at high magnification was the existence of layers surrounding the bacterial-synthesised silver nanoparticles. The aggregated nanoparticles depicted in the figure do not have direct contact with one another due to the fact that nanoparticles are stabilised by capping proteins secreted from bacteria. It is also postulated that Cytochrome C is the enzyme that may play an important role as capping agent which will affect the stability of silver nanoparticles formed by this process as the formation is quite stable for a period of five months at room ambient temperature (Abdeen et al., 2014).

(iv) Elemental composition assessment of bacterial-synthesised silver nanoparticles using EDX

The EDX microanalysis is an elemental analysis technique corresponded with electron microscopy based on the generation of characteristic X-rays that reveals the presence of elements present in the specimens. Figure 5 shows the EDX spectrum representing the elemental peak comparison of Figure 5 (A) cell-free supernatant, Figure 5 (B) $AgNO_3$ precursor, and Figure 5 (C) bacterial-synthesised silver nanoparticles. Figure 5 (D) tabulates the elemental breakdown of cell-free supernatant, $AgNO_3$ precursor and bacterial-synthesised silver nanoparticles respectively. The EDX analysis provides both qualitative and quantitative information as the position of a peak in the spectrum and its energy identifies the element as depicted in Figure 5 (A), (B) and (C).

Figure 5 (D) illustrates the EDX elemental breakdown of bacterial-synthesised silver nanoparticles comparable to cell-free supernatant and $AgNO_3$ precursor as controls in atomic percentages. The composition of cell-free supernatant mainly consists of polysaccharides and proteins as elements like C (45.03%), O (31.29%), N (15.17%), S (0.36%), and P (0.29%) with salt residues such as Na (2.35%), Cl (2.05%) and K (1.11%) present in the analysis. Chemical elements present in $AgNO_3$ precursor solutions primarily involve Ag (42.06%), followed by O (23.81%) and S (26.02%) elements. Multiple peaks such as C (3.99%), O (36.74%), S (2.57%) and Cl (4.23%) elements were present besides Ag (27.41%) in solution containing bacterial-synthesised silver nanoparticles. It was postulated that the bacterial-synthesised silver nanoparticles were surrounded by organic substances originating from cellular and media components from cell-free supernatant as the same elements but differs in atomic weight percentage were also present in the cell-free supernatant. This observation corresponded with the presence of layer covering bacterial-synthesised silver nanoparticles as shown in TEM micrograph Figure 4 (E) and (F), as the biofilm layers are the byproducts of bacterial synthesised silver nanoparticles. This discovery comparable with another study using Spirulinamethanolic extract (SME) as the TEM analysis revealed the presence of organic layer surrounding the silver nanoparticles and overall analysis results indicated that the bioactive molecules from SME would play a major role in the synthesis, capping and stabilisation of Ag^+ (LewisOscar et al., 2021). On the other hand, the presence of component C (3.99%) is from the cell-free supernatant, suggests fabrication of bacterial-synthesised silver nanoparticles. High atomic percentage of O (36.74%) are partially originated from air atmosphere (El-Saadony et al., 2019).

Elements such as S (2.57%) and Cl (4.23%) were also detected, likely indicating the presence of organic residues generated by bacteria. This observation is as supported by another study where the presence of S and Cl were reported in silver nanoparticles generated using Bacillus siamensis strain C1, isolated from the medicinal plant *Coriandrum sativum* (Ibrahim et al., 2019). Therefore, the purity of bacterial-synthesised silver nanoparticles should be improved by removing the biofilm layer surrounding nanoparticles. Al element was present in all samples as the samples were prepared on aluminium stubs prior to analysis.

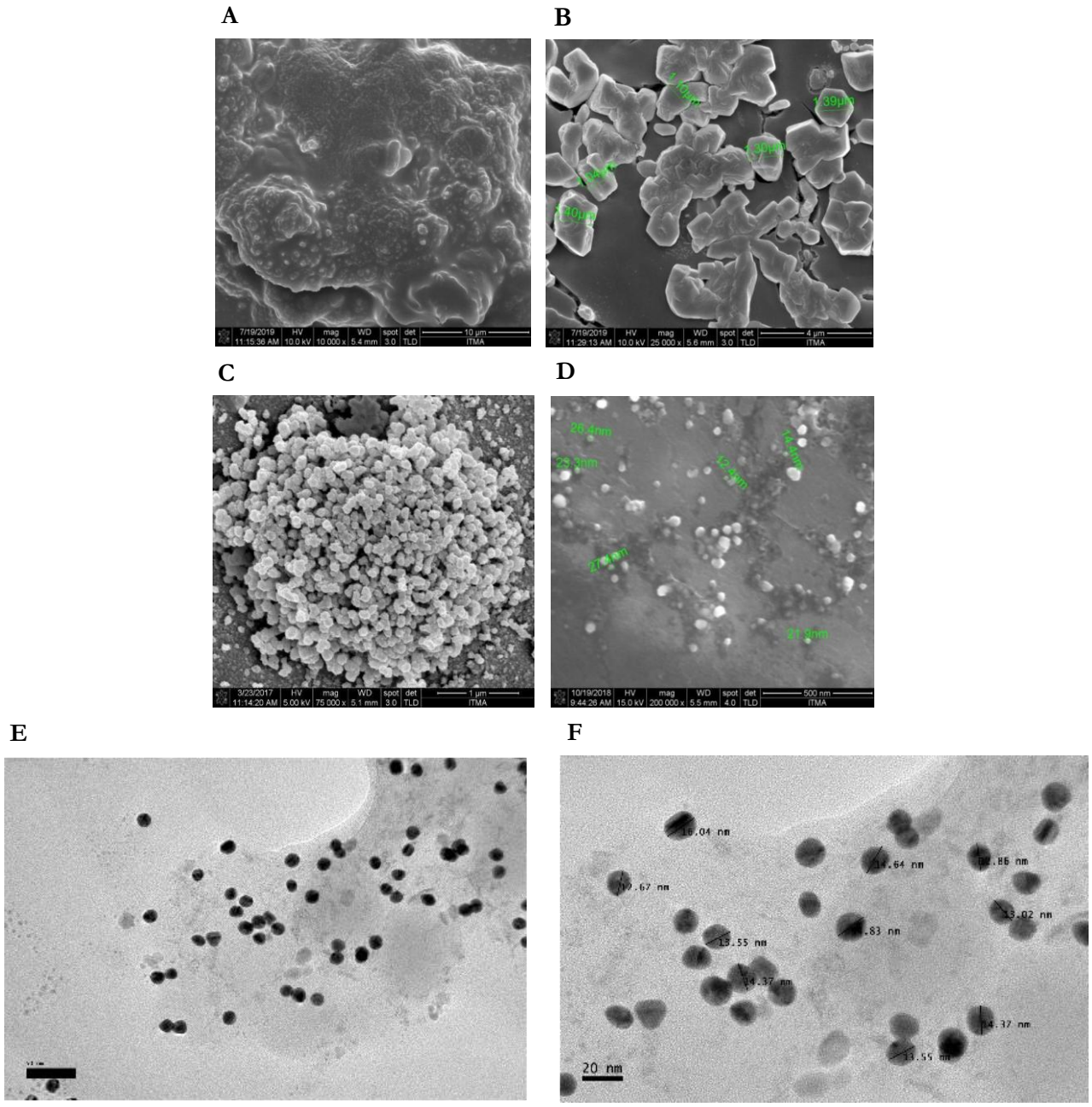

Figure 4. Morphological and particle analysis via FESEM images and TEM images. (A) demonstrated a clump and irregular shape of cell-free supernatant of silver nanoparticles-producing bacteria; (B) lattice shape of $AgNO_3$ precursor at 10 mM concentration with the size about 1 µm; (C) aggregation of bacterial-synthesised silver nanoparticles with uniform spherical shapes; (D) higher magnification of bacterial-synthesised silver nanoparticles as each nanoparticle have a diameter of less than 25 nm; (E) showed uniform and monodisperse spherical shape bacterial-synthesised silver nanoparticles surrounded by membrane-like structure produced by silver nanoparticles-producing bacteria; (F) depicting the size of bacterial-synthesised silver nanoparticles with less than 20 nm, comparable with FESEM images.

In this analysis, the amount of Ag in atomic percentage produced in bacterial-synthesised silver nanoparticles (iii) were 27.41%. Comparatively, the atomic percentage amount of Ag in another studies varies among microorganisms. For instance, biosynthesis of silver nanoparticles using strains such as E. coli, Bacillus megaterium, Acinetobacter sp. and Stenotrophomonas maltophilia resulted less than 10% of atomic percentage in Ag element (Zaki et al., 2011). Meanwhile, another study reported a high atomic percentage of Ag element at 91.80% produced by the endophytic bacterium B. siamensis strain C1 (Ibrahim et al., 2019). In comparison, a reduction of percentage atomic weight Ag was observed in bacterial-synthesised silver nanoparticles from 42.06% in solution of $AgNO_3$ precursor to 27.41% in solution of bacterial-synthesised silver nanoparticles.

In this analysis, a conversion rate of Ag elements was calculated with some modifications. The degree of conversion of silver was determined as the difference between initial concentration and the final concentration of silver (Długosz & Banach, 2019). Therefore, the conversion rate of silver amount in bacterial-synthesised silver nanoparticles was 34.83%. Referring to the conversion rate value, low yield of bacterial-synthesised silver nanoparticles is influenced by a combination of factors. Concentration of $AgNO_3$ as a precursor should be considered to increase as there are more silver ions for reduction process. However, optimal concentration range need to be determined for this specific bacterial strain as excessive substrate concentration can lead to deformed nanoparticles formation. Other than that, higher concentration of catalyst such as nitrate reductase enzymes can facilitate in reduction process more efficiently to achieve higher nanoparticles yield. This can be achieved by determining the optimal growth rate of silver nanoparticles-producing bacteria to harvest more catalyst (Ibrahim et al., 2021). However, the low rate of conversion might be attributed to bacterial species or strain that are being used to synthesise silver nanoparticles as different bacterial species or strains have varying abilities to produce silver nanoparticles. Some bacteria are naturally better suited for this process due to their specific metabolic pathways or the presence of unique enzymes. Since this silver nanoparticles-producing bacteria was naturally evolved and not–well-adapted to have nanoparticle synthesis ability may result in lower yields.

Antimicrobial potential of bacterial-synthesised silver nanoparticles

The antimicrobial potential of these bacterial-synthesised silver nanoparticles was tested against Gram-negative E. coli DH5-α using a disk diffusion assay and was found to be comparable to conventional antibiotics. Additionally, the same bacterial strain was tested in suspension to determine the growth inhibition rate of the bacterial-synthesised silver nanoparticles using a bacterial growth inhibition assay. The data obtained from these assays will be instrumental in enhancing the antimicrobial properties of bacterial-synthesised silver nanoparticles in the future, potentially broadening their effectiveness against a wider range of bacteria and other antimicrobial agents.

(i) Growth inhibition zones of E. coli treated with bacterial-synthesised silver nanoparticles

Figure 6 (A) shows the growth inhibition zones value of the disk diffusion assay to perform preliminary evaluation of the antimicrobial potential of bacterial-synthesised silver nanoparticles against gram-negative E. coli DH5α strain. Figures of the agar plate can be found in Supplementary 4. Figure 6 (B) is the secondary data generated from (A) to relatively compare the killing efficiency of silver between $AgNO_3$ precursor and bacterial-synthesised silver nanoparticles, with normalised concentration. Detailed calculations are provided in Supplementary 5. The secondary data from Figure 6 (B) was generated from the elemental composition analysis as described in Figure 5 (D). The amount of Ag in atomic weight percentage for $AgNO_3$ were not similar with the bacterial-synthesised silver nanoparticles as described in Figure 5 (D). In addition, the conversion rate of 34.83% was defined as 100% of Ag amount in $AgNO_3$ was not totally converted into bacterial-synthesised silver nanoparticles. Therefore, the secondary data from Figure 6 (B) was generated to provide a fair comparison of the antimicrobial efficiency between bacterial-synthesised silver nanoparticles and $AgNO_3$.

Based on Figure 6 (A), there was no inhibition ring exhibited on E. coli DH5α strain culture when treated with blank disk and distilled water. Similarly, there was no growth inhibition in the E. coli DH5α bacteria treated with 2 ug/mL ampicillin, indicates resistance to ampicillin based on CLSI guidelines (Adapted in part from CLSI document M100-S23 (M02-A11). This example of resistance development of E. coli DH5α to ampicillin will raise public health concern as if someone becomes infected with ampicillin-resistant bacteria, the commonly used ampicillin antibiotic will be no longer useful. The range of available treatment options becomes narrower, harder to control widespread infections and hospital treatment will be costly.

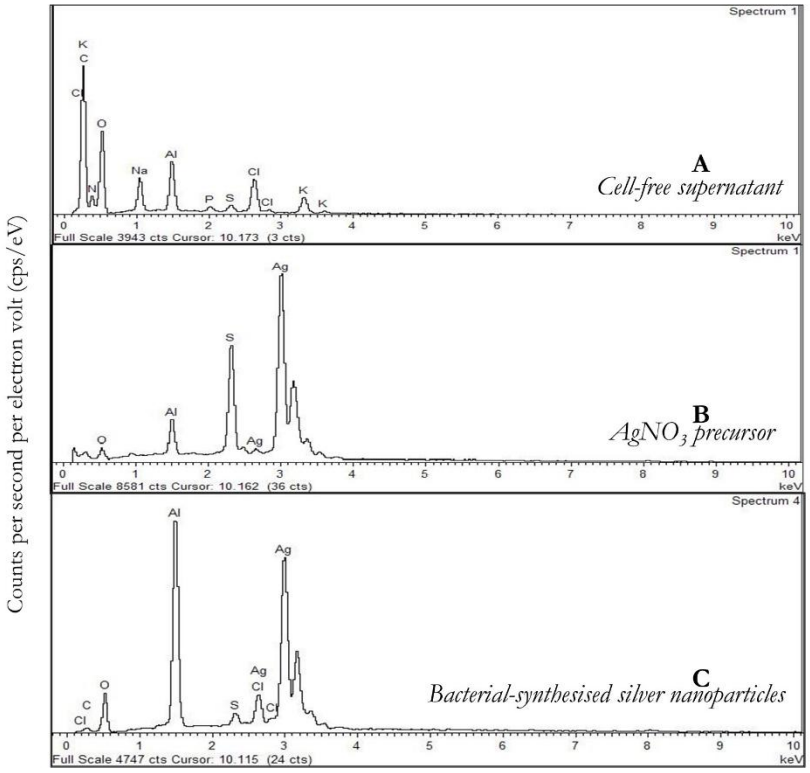

D

Elements	Atomic weight percentage (%)		
	(i) Cell-free supernatant	**(ii) $AgNO_3$ precursor**	**(iii) Bacterial-synthesised silver nanoparticles**
Carbon (C)	45.03	0.00	3.99
Nitrogen (N)	15.17	0.00	0.00
Oxygen (O)	31.29	23.81	36.74
Sodium (Na)	2.35	0.00	0.00
Aluminum (Al)	2.36	8.11	27.72
Phosphorus (P)	0.29	0.00	0.00
Sulphur (S)	0.36	26.02	2.57
Chlorine (Cl)	2.05	0.00	4.23
Potassium (K)	1.11	0.00	0.00
Silver (Ag)	0.00	42.06	27.41

Figure 5. The elemental composition of targeted samples using EDX. The elemental peaks were showed in (A) cell-free supernatant, (B) $AgNO_3$ precursor, and (C) bacterial-synthesised silver nanoparticles; (D) shows quantitative elemental breakdown comparison of bacterial-synthesised silver nanoparticles alongside with cell-free supernatant and $AgNO_3$ precursor as controls. The EDX result showed the Ag element was present together with organic residues derived from cell-free supernatant prior to generation of bacterial-synthesised silver nanoparticles.

However, the bacteria were found to be susceptible towards the other class of antibiotic used such as kanamycin at the concentration of 30 ug/mL as shown by the largest inhibition zone of 1.93±0.12 cm. Even though kanamycin has the highest antimicrobial activity, there are a few E. coli strains that are proven to confer resistance towards kanamycin. For instance, there are pathogenic strains of E. coli that can naturally exhibit resistance to kanamycin and other classes of antibiotics over time and these strains can possess significant public health concerns as limited treatment options in clinical settings. For example, some strains of Shiga toxin-producing E. coli exhibit resistance to kanamycin and have been associated with outbreaks of foodborne illness (Galarce et al., 2020). Extraintestinal pathogenic E. coli strains have been reported to be resistant to kanamycin and cause urinary tract

infections, bloodstream infections, and other infections related to gastrointestinal tract (Ukah et al., 2018). Therefore, it is crucial to find an alternative solution to overcome antimicrobial resistance.

It was known that the presence of silver in silver nanoparticles can cause disruption of cell membrane, interference with DNA replication, enzymes inhibition, and generation of reactive oxygen species (ROS) of the bacteria (Rodrigues et al., 2024). Therefore, this test is to compare the mechanistic antimicrobial action of bacterial-synthesised silver nanoparticles with Ag^+ from $AgNO_3$ precursor. The results shown in Figure 6(A) indicated an inhibition ring of 1.03±0.06 cm for the $AgNO_3$ precursor and 0.87±0.12 cm for the bacterial-synthesised silver nanoparticles. These results suggested that Ag^+ ions from the $AgNO_3$ precursor exhibit higher antimicrobial activity than the nanoscale silver in the bacterial-synthesised silver nanoparticles. However, there were reports suggesting that the inhibition effect of silvers nanoparticle were depends on the concentration of silver nanoparticle and the initial bacterial number (Dong et al., 2019; Wirth et al., 2016). After normalised the concentration between Ag^+ from $AgNO_3$ and silver nanoparticles, the antimicrobial activity efficiency of bacterial-synthesised silver nanoparticles are superior than $AgNO_3$ precursor as shown in Figure 6 (B), given normalised concentration in millimolar (mM) and the signs of asterisks (*) are the calculated data. The initial concentration (mM) was derived from the conversion rate as described in methodology. In the same 10 mM concentration of $AgNO_3$ precursor and bacterial-synthesised silver nanoparticles, the bacterial-synthesised silver nanoparticles confer a higher zone of inhibition of 2.58 cm (calculated data) than $AgNO_3$ precursor at 1.03 cm zone of inhibition. The same trend was observed in 3.48 mM concentration, as the larger inhibition zone of 0.9 cm in bacterial-synthesised silver nanoparticles than $AgNO_3$ precursor, which only 0.36 cm (Figure 6B).

Subsequently, the rate of killing efficiency of bacterial-synthesised silver nanoparticles was 150.5% which also means 1.5 times higher than non-nano silver in $AgNO_3$ precursor. This is due to the extremely small size in nano-dimension of silver, with larger surface area per volume ratio, so more atoms can interact with bacteria and subsequently enhance the superior antimicrobial properties of silver comparative to different mechanism of action as the presence of Ag^+ ions induced by $AgNO_3$. A comparison study of mechanism of actions between chemically-synthesised silver nanoparticles (8 and 29 nm) and $AgNO_3$ with the same concentrations of 10μg/mL was also conducted. However, there are no inhibition zones observed in different E. coli (Trans 1-T1) strain when treated with 8 and 29 nm of chemically-synthesised silver nanoparticles while 10 mm of inhibition zone was recorded when the bacteria treated with $AgNO_3$ (Mosselhy et al., 2015). This project can be advantageous and high potential as the bacterial-synthesised silver nanoparticles still have the antimicrobial effect towards gram-negative E. coli, but the establishment of the test need to be done by normalising and widening the concentration range, together with antimicrobial assessment with wide-range of bacteria. Next, the susceptibility profile of E. coli DH5-α was evaluated using the CLSI M100 guideline, which helped classify the organisms as susceptible, intermediate, or resistant to each antimicrobial agent tested, based on the various interpretative criteria for susceptibility.

(ii) Bacterial growth inhibition assay

In this assay, lag phase and log phage cells were examined to assess the effect of nanoparticles on cell doubling and suppression of bacterial proliferation, respectively. In both tests, E. coli DH5-α were treated with different concentration of nanoparticles, with raw result data in Supplementary 6. Referring to Figure 7(A), the bacterial culture treated with 1% (v/v) bacterial-synthesised silver nanoparticles in both the lag and log phases showed a non-significant increase in bacterial growth, despite having a higher OD reading than the untreated control culture. This might due to the negligible 1% (v/v) concentration which has no effect on the bacterial growth. However, when the concentration of bacterial-synthesised silver nanoparticles was increased to 10% (v/v), bacterial growth was inhibited by 50% in comparison to the normal growth curve. This indicates that 10% (v/v) concentration is enough to inhibit the growth of bacteria in suspension as OD increased is significantly less than 1% treatment in both lag and log phases as shown in Figure 7(B). From this study, the low concentration of 1% (v/v) did not affect the growth of the bacteria. This might due to the low amount of atomic weight percentage and conversion rate of silver in bacterial-synthesised silver nanoparticles comparable to silver in $AgNO_3$ as discussed in Figure 5 (D). This observation aligns with a study evaluating E. coli and B. subtilis growth using chemically-synthesised citrate-capped silver nanoparticles at different concentrations of 10, 30, and 50 mg/mL. In E. coli, it shows a similar concentration-dependent response as observed in this assay. However, B. subtilis showed less susceptibility, likely due to its thicker peptidoglycan layer (Kim et al., 2011). Comparatively, the growth of Cupriavidus necator H16 was evaluated when treated with spherical silver nanoparticles. Low amount of 20 μg/mL of silver nanoparticles did not have any effect

on the growth of C. necator. However, when the concentration of silver nanoparticles was increased to 60 μg/mL, the growth in C. necator cultures was significantly inhibited (Schacht et al., 2013). Another similar observation was reported, where a high concentration of bacterial-synthesised silver nanoparticles significantly reduced the growth rate of E. coli compared to a lower concentration, which aligns with the results obtained in this assay (Bao et al., 2015). Possible inhibition mechanism of bacterial-synthesised silver nanoparticles in suspension culture is due to the aggregation surrounding bacteria cells followed by nanoparticles uptake and dissolution of Ag^+ to disrupt the cell membrane comparing to the effect on direct Ag^+ in silver alone. This was proven by the electron microscopy micrograph picturing the accumulation of silver nanoparticles covering the membrane of the bacteria (Kim et al., 2011).

A

Testing agents	Inhibition zone (cm) *E. coli* DH5α				
	R1	R2	R3	Mean	SD
Blank disk	0.00	0.00	0.00	0.00	0.00
Distilled water	0.00	0.00	0.00	0.00	0.00
Ampicillin (2 ug/mL)	0.00	0.00	0.00	0.00	0.00
Kanamycin (30 ug/mL)	1.80	2.00	2.00	1.93	0.12
$AgNO_3$ precursor (10 mM)	1.00	1.00	1.10	1.03	**** 0.06
AgNPs (500μL)	0.80	0.80	1.00	0.87	**** 0.12

Clinical and Laboratory Standards Institute (CLSI) guidelines

Antibiotic (ug)	Test Cultures (zone diameters in mm)		
	Resistant	Intermediate	Susceptible
Ampicillin (10 ug)	≤13	14-16	≥17
Kanamycin (30 ug)	≤13	14-17	≥18

*Adapted in part from CLSI document M100-S23 (M02-A11): Performance standards for antimicrobial susceptibility testing

B

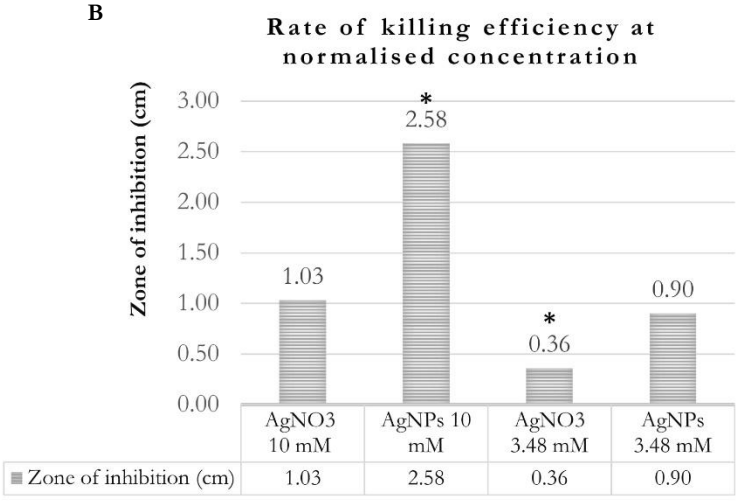

Asterisk (*) symbol represents calculated data

Figure 6. Antibacterial evaluation of bacterial–synthesised silver nanoparticles. (A) quantitative data of the disk diffusion assay in triplicate against *E. coli* DH5α strain as there was no growth inhibition in *E. coli* DH5α when tested with negative controls such as blank disk and distilled water together with ampicillin (2 ug/mL). Kanamycin (30 ug/mL) possessed the largest inhibition zone 1.93±0.12 cm followed by $AgNO_3$ precursor (10 mM) and bacterial-synthesised silver nanoparticles. Statistical analysis was conducted to compare the effects of treatment with silver nanoparticles to those of distilled water (Negative control). "*" indicates significance with $p < 0.05$; "**": $p < 0.01$; "***": $p < 0.001$; $p < 0.0001$ and ns: not significant. (B) is the comparison of killing efficiency rate between $AgNO_3$ ($AgNO_3$ precursor) and AgNPs (bacterial-synthesised silver nanoparticles), given the normalised concentration. It is postulated that the killing efficiency of silver contained in bacterial-synthesised silver nanoparticles is higher than in $AgNO_3$ precursor because of the distinct nano dimensions of bacterial-synthesised silver nanoparticles which contributes to higher efficiency rate of killing.

Predictably, higher content of Ag in atomic weight percentage in bacterial-synthesised silver nanoparticles to inhibit the growth of targeted bacteria cells. However, it is important to determine the optimal concentration used, especially in biomedical applications as toxicity results should be conducted carefully to be suitable alternative to other therapeutics. In addition, the environment in which nanoparticles are exposed can influence their properties and, consequently, their antimicrobial activity. In both assays, the bacterial-synthesised silver nanoparticles have been exposed to LB medium, which contain electrolytes comparing with distilled water. Previous study reported that the presence of salts such as potassium chloride and sodium chloride in growth media induced the aggregation of nanoparticles and forming clusters immediately, which changes their size and surface properties (Meyer et al., 2010). The aggregation caused by the salts in the LB medium might enhance the nanoparticles' interactions with bacterial cell walls, possibly due to larger clusters being more reactive in this environment. The hydrodynamic diameter of silver nanoparticles in LB medium was also recorded in DLS to be two to three times greater than the hydrodynamic diameter of silver nanoparticles in water (Kim et al., 2011). Therefore, the aggregation and size increase due to the electrolytes in LB medium influence the nanoparticles' surface area, reactivity, and interaction with microbes, potentially enhancing their antimicrobial action.

CONCLUSION

The silver nanoparticle-producing bacteria were identified as closely related to *Bacillus* strains by phylogenetic analysis. UV-vis spectrometry showed a peak at 420 nm, confirming nanoparticle synthesis, while DLS revealed an average size of 139.73 nm, and electron microscopy confirmed nanoparticles were less than 25 nm, surrounded by biofilm layers. Antimicrobial tests demonstrated that the nanoparticles inhibited *E. coli* DH5-α growth by 50% at a 10% concentration and were 1.5 times more effective than $AgNO_3$ at normalised concentration, suggesting their potential to complement antibiotics in addressing antimicrobial resistance.

ACKNOWLEDGEMENTS

The author thanks Assoc. Prof. Dr. Mas Jaffri Masarudin, Dr. Patricia Jayshree Samuel Jacob, and Prof. Dr. Rosfarizan Mohamad for their conceptualisation and validation of the study; Chew Xin Jie for assisting in research investigation; Dr Tham Hong Yun for assisting in manuscript editing; and Assoc. Prof. Mas Jaffri Masarudin for supervision, review, and manuscript editing. All authors have reviewed and approved the final version of the manuscript. This project was funded by the Universiti Putra Malaysia research grant (Geran Putra, vote number 9582100). The author received financial support through a Graduate Research Fellowship (GRF) from Universiti Putra Malaysia.

CONFLICT OF INTEREST

The authors have declared that no conflict of interest exists.

REFERENCES

Abdeen, S., Geo, S., Praseetha, P. K., & Dhanya, R. P. (2014). Biosynthesis of silver nanoparticles from *Actinomycetes* for therapeutic applications. *International Journal of Nano Dimension*, *5*(2): 155-162. https://www.sid.ir/paper/322131/fa

Abram, S.-L., & Fromm, K. M. (2020). Handling (Nano)Silver as antimicrobial agent: therapeutic window, dissolution dynamics, detection methods and molecular interactions. *Chemistry – A European Journal*, *26*(48), 10948–10971. https://doi.org/10.1002/chem.202002143

Ahmed, T., & Ogulata, R. T. (2022). A review on silver nanoparticles -green synthesis, antimicrobial action and application in textiles. *Journal of Natural Fibers*. *19*(14), 8463-8484. https://doi.org/10.1080/15440478.2021.1964135

Alotaibi, B. S., Khan, M., & Shamim, S. (2021). Unraveling the underlying heavy metal detoxification mechanisms of *Bacillus* species. *Microorganisms*, *9*(8), 1628. https://doi.org/10.3390/microorganisms9081628

Avershina, E., Shapovalova, V., & Shipulin, G. (2021). Fighting antibiotic resistance in hospital-acquired infections: current state and emerging technologies in disease prevention, diagnostics and therapy. *Frontiers in Microbiology*, *12*, 707330. https://doi.org/10.3389/fmicb.2021.707330

Babu, M. G., & Gunasekaran, P. (2009). Production and structural characterization of crystalline silver nanoparticles from *Bacillus cereus* isolate. *Colloids and Surfaces B: Biointerfaces*, *74*(1), 191–195. https://doi.org/10.1016/j.colsurfb.2009.07.016

Bao, H., Yu, X., Xu, C., Li, X., Li, Z., Wei, D., & Liu, Y. (2015). New toxicity mechanism of silver nanoparticles: Promoting apoptosis and inhibiting proliferation. *PLoS One*, *10*(3), e0122535. https://doi.org/10.1371/journal.pone.0122535

Barani, H., & Mahltig, B. (2022). Microwave-assisted synthesis of silver nanoparticles: Effect of reaction temperature and precursor concentration on

fluorescent property. *Journal of Cluster Science*, *33*(1), 101–111. https://doi.org/10.1007/s10876-020-01945-x

Beyene, H. D., Werkneh, A. A., Bezabh, H. K., & Ambaye, T. G. (2017). Synthesis paradigm and applications of silver nanoparticles (AgNPs), a review. *Sustainable Materials and Technologies*, *13*, 18–23. https://doi.org/10.1016/j.susmat.2017.08.001

Bu, Y., & Lee, S. (2012). Influence of dopamine concentration and surface coverage of Au shell on the optical properties of Au, Ag, and Ag $_{\text{core}}$ Au $_{\text{shell}}$ nanoparticles. *ACS Applied Materials & Interfaces*, *4*(8), 3923–3931. https://doi.org/10.1021/am300750s

Chandrakanth, R. K., Ashajyothi, C., Oli, A. K., & Prabhurajeshwar, C. (2014). Potential bactericidal effect of silver nanoparticles synthesised from *Enterococcus* species. *Oriental Journal of Chemistry*, *30*, 3. http://dx.doi.org/10.13005/ojc/300341

Das, C. G. A., Kumar, V. G., Dhas, T. S., Karthick, V., Govindaraju, K., Joselin, J. M., & Baalamurugan, J. (2020). Antibacterial activity of silver nanoparticles (biosynthesis): A short review on recent advances. *Biocatalysis and Agricultural Biotechnology*, *27*, 101593. https://doi.org/10.1016/j.bcab.2020.101593

Dave, A., Sharma, K., & Sharma, C. R. (2022). Green synthesis and standardization of biologically synthesized silver nanoparticles. *Research Journal of Pharmacy and Technology*, *15*(2), 870–872. DOI: 10.52711/0974-360X.2022.00145

Długosz, O., & Banach, M. (2019). Continuous production of silver nanoparticles and process control. *Journal of Cluster Science*, *30*(3), 541–552. https://doi.org/10.1007/s10876-019-01505-y

Dong, Y., Zhu, H., Shen, Y., Zhang, W., & Zhang, L. (2019). Antibacterial activity of silver nanoparticles of different particle size against *Vibrio Natriegens*. *PLOS ONE*, *14*(9), e0222322. https://doi.org/10.1371/journal.pone.0222322

Eaton, P., Quaresma, P., Soares, C., Neves, C., De Almeida, M. P., Pereira, E., & West, P. (2017). A direct comparison of experimental methods to measure dimensions of synthetic nanoparticles. *Ultramicroscopy*, *182*, 179–190. https://doi.org/10.1016/j.ultramic.2017.07.001

Egerton, R. F. (2011). An introduction to EELS. In R. F. Egerton (Ed.), Electron energy-loss spectroscopy in the electron microscope (pp. 1–28). Springer US. https://doi.org/10.1007/978-1-4419-9583-4_1

El-Saadony, M. T., El-Wafai, N. A., El-Fattah, H. I. A., & Mahgoub, S. A. (2019). Biosynthesis, optimization and characterization of silver nanoparticles using a soil isolate of *Bacillus pseudomycoides* MT32 and their antifungal activity against some pathogenic fungi. *Advances in Animal and Veterinary Sciences*, *7*(4), 238–249. http://dx.doi.org/10.17582/journal.aavs/2019/7.4.238.249

Endres, S. C., Ciacchi, L. C., & Mädler, L. (2021). A review of contact force models between nanoparticles in agglomerates, aggregates, and films. *Journal of Aerosol Science*, *153*, 105719. https://doi.org/10.1016/j.jaerosci.2020.105719

Gade, A. K., Bonde, P., Ingle, A. P., Marcato, P. D., Duran, N., & Rai, M. K. (2008). Exploitation of *Aspergillus niger* for synthesis of silver nanoparticles. *Journal of Biobased Materials and Bioenergy*, *2*(3), 243–247. https://doi.org/10.1166/jbmb.2008.401

Galarce, N., Sánchez, F., Fuenzalida, V., Ramos, R., Escobar, B., Lapierre, L., Paredes-Osses, E., Arriagada, G., Alegría-Morán, R., Lincopán, N., Fuentes-Castillo, D., Vera-Leiva, A., González-Rocha, G., Bello-Toledo, H., & Borie, C. (2020). Phenotypic and genotypic antimicrobial resistance in non-O157 Shiga toxin-producing *Escherichia coli* isolated from cattle and swine in Chile. *Frontiers in Veterinary Science*, *7*(367). https://doi.org/10.3389/fvets.2020.00367

Ghareib, M., Tahon, M. A., Saif, M. M., & El-Sayed Abdallah, W. (2016). Rapid extracellular biosynthesis of silver nanoparticles by *Cunninghamella phaeospora* culture supernatant. *Iranian Journal of Pharmaceutical Research*, *15*(4), 915–924.

Gherasim, O., Puiu, R. A., Bîrcă, A. C., Burduşel, A.-C., & Grumezescu, A. M. (2020). An updated review on silver nanoparticles in biomedicine. *Nanomaterials*, *10*(11), 2318. https://doi.org/10.3390/nano10112318

Ghorbani, H. R. (2013). Biosynthesis of silver nanoparticles using *Salmonella typhirium*. *Journal of Nanostructure in Chemistry*, *3*(1), 29. https://doi.org/10.1186/2193-8865-3-29

Gomes, T. A., Zanette, C. M., & Spier, M. R. (2020). An overview of cell disruption methods for intracellular biomolecules recovery. *Preparative Biochemistry & Biotechnology*, *50*(7), 635–654. https://doi.org/10.1080/10826068.2020.1728696

Ibrahim, E., Fouad, H., Zhang, M., Zhang, Y., Qiu, W., Yan, C., Li, B., Mo, J., & Chen, J. (2019). Biosynthesis of silver nanoparticles using endophytic bacteria and their role in inhibition of rice pathogenic bacteria and plant growth promotion. *RSC Advances*, *9*(50), 29293–29299. DOI: 10.1039/c9ra04246f

Ibrahim, S., Ahmad, Z., Manzoor, M. Z., Mujahid, M., Faheem, Z., & Adnan, A. (2021). Optimization for biogenic microbial synthesis of silver nanoparticles through response surface methodology, characterization, their antimicrobial, antioxidant, and catalytic potential. *Scientific Reports*, *11*(1), 770. https://doi.org/10.1038/s41598-020-80805-0

Jadoun, S., Chauhan, N. P. S., Zarrintaj, P., Barani, M., Varma, R. S., Chinnam, S., & Rahdar, A. (2022). Synthesis of nanoparticles using microorganisms and their applications: A review. *Environmental Chemistry Letters*, *20*(5), 3153–3197. https://doi.org/10.1007/s10311-022-01444-7

Kalai Priya, A., Yogesh, G. K., Subha, K., Kalyanavalli, V., & Sastikumar, D. (2021). Synthesis of silver nano-butterfly park by using laser ablation of aqueous salt for gas sensing application. *Applied Physics A*, *127*(4), 292. https://doi.org/10.1007/s00339-021-04370-7

Kalimuthu, K., Babu, R. S., Venkataraman, D., Bilal, M., & Gurunathan, S. (2008). Biosynthesis of silver nanocrystals by *Bacillus licheniformis*. *Colloids and*

Surfaces B: Biointerfaces, *65*(1), 150–153. https://doi.org/10.1016/j.colsurfb.2008.02.018

Kamala Nalini, S. P., & Vijayaraghavan, K. (2020). Green synthesis of silver and gold nanoparticles using Aloe vera gel and determining its antimicrobial properties on nanoparticle impregnated cotton fabric. *Journal of Nanotechnology Research*, *2*(3), 42–50. DOI: 10.26502/jnr.2688-85210015

Kim, S. W., Baek, Y.-W., & An, Y.-J. (2011). Assay-dependent effect of silver nanoparticles to *Escherichia coli* and *Bacillus subtilis*. *Applied Microbiology and Biotechnology*, *92*(5), 1045–1052. https://doi.org/10.1007/s00253-011-3611-x

Kweon, O. J., Lim, Y. K., Kim, H. R., Kim, T.-H., Ha, S., & Lee, M.-K. (2020). Isolation of a novel species in the genus *Cupriavidus* from a patient with sepsis using whole genome sequencing. *PLOS ONE*, *15*(5), e0232850. https://doi.org/10.1371/journal.pone.0232850

Lee, S. H., & Jun, B.-H. (2019). Silver nanoparticles: synthesis and application for nanomedicine. *International Journal of Molecular Sciences*, *20*(4), 865. https://doi.org/10.3390/ijms20040865

LewisOscar, F., Nithya, C., Vismaya, S., Arunkumar, M., Pugazhendhi, A., Nguyen-Tri, P., Alharbi, S. A., Alharbi, N. S., & Thajuddin, N. (2021). In vitro analysis of green fabricated silver nanoparticles (AgNPs) against *Pseudomonas aeruginosa* PA14 biofilm formation, their application on urinary catheter. *Progress in Organic Coatings*, *151*, 106058. https://doi.org/10.1016/j.porgcoat.2020.106058

Linhares, A. M. F., Borges, C. P., & Fonseca, F. V. (2020). Investigation of biocidal effect of microfiltration membranes impregnated with silver nanoparticles by sputtering technique. *Polymers*, *12*(8), 1686. https://doi.org/10.3390/polym12081686

Link, S., & El-Sayed, M. A. (2003). Optical properties and ultrafast dynamics of metallic nanocrystals. *Annual Review of Physical Chemistry*, *54*, 331–366. https://doi.org/10.1146/annurev.physchem.54.011002.103759

Mat Lazim, Z., Salmiati, S., Marpongahtun, M., Arman, N. Z., Mohd Haniffah, M. R., Azman, S., Yong, E. L., & Salim, M. R. (2023). Distribution of silver (Ag) and silver nanoparticles (AgNPs) in aquatic environment. *Water*, *15*(7), 349. https://doi.org/10.3390/w15071349

Mathivanan, K., Selva, R., Chandirika, J. U., Govindarajan, R. K., Srinivasan, R., Annadurai, G., & Duc, P. A. (2019). Biologically synthesized silver nanoparticles against pathogenic bacteria: Synthesis, calcination and characterization. *Biocatalysis and Agricultural Biotechnology*, *22*, 101373. https://doi.org/10.1016/j.bcab.2019.101373

Meyer, J. N., Lord, C. A., Yang, X. Y., Turner, E. A., Badireddy, A. R., Marinakos, S. M., Chilkoti, A., Wiesner, M. R., & Auffan, M. (2010). Intracellular uptake and associated toxicity of silver nanoparticles in *Caenorhabditis elegans*. *Aquatic Toxicology*, *100*(2), 140–150. https://doi.org/10.1016/j.aquatox.2010.07.016

Modi, S., Pathak, B., & Fulekar, M. H. (2015). Microbial synthesized silver nanoparticles for decolorization and biodegradation of azo dye compound. *Journal of Environmental Nanotechnology*, *4*(2), 37–46. doi:10.13074/jent.2015.06.152149

Mosselhy, D. A., El-Aziz, M. A., Hanna, M., Ahmed, M. A., Husien, M. M., & Feng, Q. (2015). Comparative synthesis and antimicrobial action of silver nanoparticles and silver nitrate. *Journal of Nanoparticle Research*, *17*(12), 473. https://doi.org/10.1007/s11051-015-3279-8

Mustapha, T., Misni, N., Ithnin, N. R., Daskum, A. M., & Unyah, N. Z. (2022). A review on plants and microorganisms mediated synthesis of silver nanoparticles, role of plants metabolites and applications. *International Journal of Environmental Research and Public Health*, *19*(2), 674. https://doi.org/10.3390/ijerph19020674

Nguyen, N. P. U., Dang, N. T., Doan, L., & Nguyen, T. T. H. (2023). Synthesis of silver nanoparticles: from conventional to 'modern' methods—a review. *Processes*, *11*(9), 2617. https://doi.org/10.3390/pr11092617

Pan, N., Wei, Y., Zuo, M., Li, R., Ren, X., & Huang, T.-S. (2020). Antibacterial poly (ε-caprolactone) fibrous membranes filled with reduced graphene oxide-silver. *Colloids and Surfaces A: Physicochemical and Engineering Aspects*, *603*, 125186. https://doi.org/10.1016/j.colsurfa.2020.125186

Patel, J. K., Patel, A., & Bhatia, D. (2021). Introduction to nanomaterials and nanotechnology. In J. K. Patel & Y. V. Pathak (Eds.), Emerging technologies for nanoparticle manufacturing (pp. 3–23). Springer International Publishing. https://doi.org/10.1007/978-3-030-50703-9_1

Pourali, P., & Yahyaei, B. (2016). Biological production of silver nanoparticles by soil isolated bacteria and preliminary study of their cytotoxicity and cutaneous wound healing efficiency in rat. *Journal of Trace Elements in Medicine and Biology*, *34*, 22–31. https://doi.org/10.1016/j.jtemb.2015.11.004

Prabhakaran, K., Nagarajan, R., Merlin Franco, F., & Anand Kumar, A. (2017). Biomonitoring of Malaysian aquatic environments: A review of status and prospects. *Ecohydrology & Hydrobiology*, *17*(2), 134–147. https://doi.org/10.1016/j.ecohyd.2017.03.001

Raju, D., Mehta, U. J., & Ahmad, A. (2015). Simple recovery of intracellular gold nanoparticles from peanut seedling roots. *Journal of Nanoscience and Nanotechnology*, *15*(2), 1575–1581. https://doi.org/10.1166/jnn.2015.9046

Ramalingam, V., Rajaram, R., PremKumar, C., Santhanam, P., Dhinesh, P., Vinothkumar, S., & Kaleshkumar, K. (2014). Biosynthesis of silver nanoparticles from deep sea bacterium *Pseudomonas aeruginosa* JQ989348 for antimicrobial, antibiofilm, and cytotoxic activity. *Journal of Basic Microbiology*, *54*(9), 928–936. https://doi.org/10.1002/jobm.201300514

Ramamurthy, T., Ghosh, A., Chowdhury, G., Mukhopadhyay, A. K., Dutta, S., & Miyoshi, S. (2022). Deciphering the genetic network and

programmed regulation of antimicrobial resistance in bacterial pathogens. *Frontiers in Cellular and Infection Microbiology*, *12*, 952491. https://doi.org/10.3389/fcimb.2022.952491

Rodrigues, A. S., Batista, J. G. S., Rodrigues, M. Á. V., Thipe, V. C., Minarini, L. A. R., Lopes, P. S., & Lugão, A. B. (2024). Advances in silver nanoparticles: A comprehensive review on their potential as antimicrobial agents and their mechanisms of action elucidated by proteomics. *Frontiers in Microbiology*, *15*. https://doi.org/10.3389/fmicb.2024.1440065

Rodriguez-Iruretagoiena, A., Graham, M., Gredilla, A., Fdez-Ortiz de Vallejuelo, S., Cornelis, G., Schulte-Herbrüggen, H., Madariaga, J. M., & de Diego, A. (2022). A new procedure to quantify silver nanoparticles in sediments. *Gondwana Research*, *110*, 264–269. https://doi.org/10.1016/j.gr.2021.07.012

Sadhasivam, S., Shanmugam, P., & Yun, K. (2010). Biosynthesis of silver nanoparticles by *Streptomyces hygroscopicus* and antimicrobial activity against medically important pathogenic microorganisms. *Colloids and Surfaces B: Biointerfaces*, *81*(1), 358–362. https://doi.org/10.1016/j.colsurfb.2010.07.036

Saeed, S., Iqbal, A., & Ashraf, M. A. (2020). Bacterial-mediated synthesis of silver nanoparticles and their significant effect against pathogens. *Environmental Science and Pollution Research*, *27*(30), 37347–37356. https://doi.org/10.1007/s11356-020-07610-0

Schacht, V. J., Neumann, L. V., Sandhi, S. K., Chen, L., Henning, T., Klar, P. J., Theophel, K., Schnell, S., & Bunge, M. (2013). Effects of silver nanoparticles on microbial growth dynamics. *Journal of Applied Microbiology*, *114*(1), 25–35. https://doi.org/10.1111/jam.12000

Selvam, A., Sharma, R., Sutradhar, S., & Chakrabarti, S. (2021). Synthesis of carbon allotropes in nanoscale regime. In A. Hazra & R. Goswami (Eds.), Carbon nanomaterial electronics: devices and applications (pp. 9–46). Springer. https://doi.org/10.1007/978-981-16-1052-3_2

Shivaji, S., Madhu, S., & Singh, S. (2011). Extracellular synthesis of antibacterial silver nanoparticles using psychrophilic bacteria. *Process Biochemistry*, *46*(9), 1800–1807. https://doi.org/10.1016/j.procbio.2011.06.008

Silva, C. D., Noor, A. A. M., Karim, M. M. A., Gunasekaran, B., Gani, S. A., Cabrera, M. A., & Ahmad, S. A. (2020). The green synthesis and characterisation of silver nanoparticles from Serratia spp Síntesis verde y caracterización de nanopartículas de plata de Serratia spp. *Revista Mexicana de Ingeniería Química* 19(3): 1327-1339. https://doi.org/10.24275/rmiq/Bio1059

Smitha, S. L., Nissamudeen, K. M., Philip, D., & Gopchandran, K. G. (2008). Studies on surface plasmon resonance and photoluminescence of silver nanoparticles. *Spectrochimica Acta Part A: Molecular and Biomolecular Spectroscopy*, *71*(1), 186–190. https://doi.org/10.1016/j.saa.2007.12.002

Soltys, L., Olkhovyy, O., Tatarchuk, T., & Naushad, M. (2021). Green synthesis of metal and metal oxide nanoparticles: principles of green chemistry and raw materials. *Magnetochemistry*, *7*(11),145. https://doi.org/10.3390/magnetochemistry7110145

Tatarchuk, V. V., Sergievskaya, A. P., Korda, T. M., Druzhinina, I. A., & Zaikovsky, V. I. (2013). Kinetic factors in the synthesis of silver nanoparticles by reduction of Ag^{+} with hydrazine in reverse micelles of Triton N-42. *Chemistry of Materials*, *25*(18), 3570–3579. https://doi.org/10.1021/cm304115j

Ukah, U. V., Glass, M., Avery, B., Daignault, D., Mulvey, M. R., Reid-Smith, R. J., Parmley, E. J., Portt, A., Boerlin, P., & Manges, A. R. (2018). Risk factors for acquisition of multidrug-resistant *Escherichia coli* and development of community-acquired urinary tract infections. *Epidemiology & Infection*, *146*(1), 46–57. https://doi.org/10.1017/S0950268817002680

Verma, S. K., Jha, E., Panda, P. K., Mishra, A., Thirumurugan, A., Das, B., Parashar, S. K. S., & Suar, M. (2018). Rapid novel facile biosynthesized silver nanoparticles from bacterial release induce biogenicity and concentration dependent *in vivo* cytotoxicity with embryonic zebrafish—A mechanistic insight. *Toxicological Sciences*, *161*(1), 125–138. https://doi.org/10.1093/toxsci/kfx204

Wirth, S. M., Bertuccio, A. J., Cao, F., Lowry, G. V., & Tilton, R. D. (2016). Inhibition of bacterial surface colonization by immobilized silver nanoparticles depends critically on the planktonic bacterial concentration. *Journal of Colloid and Interface Science*, *467*, 17–27. https://doi.org/10.1016/j.jcis.2015.12.049

Xin, X., Qi, C., Xu, L., Gao, Q., & Liu, X. (2022). Green synthesis of silver nanoparticles and their antibacterial effects. *Frontiers in Chemical Engineering*, *4*. https://doi.org/10.3389/fceng.2022.941240

Xu, L., Wang, Y.-Y., Huang, J., Chen, C.-Y., Wang, Z.-X., & Xie, H. (2020). Silver nanoparticles: Synthesis, medical applications and biosafety. *Theranostics*, *10*(20), 8996–9031. https://doi.org/10.7150/thno.45413

Zaki, S., El Kady, M. F., & Abd-El-Haleem, D. (2011). Biosynthesis and structural characterization of silver nanoparticles from bacterial isolates. *Materials Research Bulletin*, *46*(10), 1571–1576. https://doi.org/10.1016/j.materresbull.2011.06.025

Zhu, Y., Huang, W. E., & Yang, Q. (2022). Clinical perspective of antimicrobial resistance in bacteria. *Infection and Drug Resistance*, *15*, 735–746. https://doi.org/10.2147/IDR.S345574